Phys. Lett. B 872 (2026) 140084

Contents lists available at ScienceDirect

Physics Letters B

journal homepage: www.elsevier.com/locate/physletb

Letter

Fusion of $^{12}C + ^{28}Si$ at deep sub-barrier energies

A. M. Stefanini [a,*], G. Montagnoli [b,c], M. Del Fabbro [b,c], A. Goasduff [a], P. A. Aguilera Jorquera [b,c], G. Andreetta [b,c], F. Angelini [a,b], L. V. D'Auria [b], M. Balogh [a], D. Bazzacco [c], J. Benito [b,c], G. Benzoni [d], M. A. Bentley [e], N. Bez [c], A. Bonhomme [f], S. Bottoni [d,g], A. Bracco [d,g], D. Brugnara [a], L. Busak [h], S. Capra [d], S. Carollo [b,c], S. Casans [i], E. Clément [j], P. Cocconi [a], A. Cogo [a], G. Colucci [k], A. Conte [a], E. Coradin [b], L. Corradi [a], S. Courtin [f], G. Deangelis [a], J. M. Deltoro [l], G. Del Piero [b], R. Depalo [d,g], J. Dudouet [m], A. Ertoprak [a], E. Fioretto [a], A. Gadea [k], F. Galtarossa [b,c], A. Gambalonga [a], A. Giaz [d], B. Gongora Servin [a,n], V. González [i], A. Gottardo [a], A. Gozzelino [a], G. Harmant [f], M. Heine [f], I. Kuti [o], M. Labiche [p], S.M. Lenzi [b,c], S. Leoni [d,f], M. Mazzocco [b,c], R. Menegazzo [c], D. Mengoni [b,c], T. Mijatović [h], B. Million [d], E. Monpribat [f], A. Nannini [q], D. R. Napoli [a], A. E. Navarro-Antón [i], R. Nicolas Del Alamo [b,c], J. Nyberg [r], S. Paschalis [e], J. Pellumaj [b,c], R. M. Pérez-Vidal [a,l], M. Petri [e], E. Pilotto [b,c], S. Pigliapoco [b,c], Z. S. Podolyak [s], M. Polettini [b,c], A. Pullia [d,g], L. Ramina [c], M. Rampazzo [c], W. Raniero [a], M. Rebeschini [c], F. Recchia [b,c], P. Reiter [t], K. Rezynkina [b,c], M. Rocchini [q], D. Rosso [a], E. Sanchis [i], M. Scarcioffolo [b], D. Scarpa [a], M. Şenyiğit [u], J. Simpson [p], D. Sohler [o], O. Stezowski [m], D. Stramaccioni [a,b], S. Szilner [h], C. Theisen [v,1], N. Toniolo [a], A. Trzcinska [k], J. J. Valiente Dobon [l], F. Veronese [c], J. Vesic [w], V. Volpe [a], K. Wimmer [x], L. Zago [a,g], I. Zanon [y], M. Zielińska [v]

[a] INFN, Laboratori Nazionali di Legnaro, Legnaro, I-35020, Italy
[b] Department of Physics and Astronomy, University of Padua, Padua, I-35020, Italy
[c] INFN, Section of Padua, Padua, I-35020, Italy
[d] INFN, Section of Milan, Milan, I-20133, Italy
[e] School of Physics, Engineering and Technology, University of York, Heslington, York, YO10 5DD, UK
[f] University of Strasbourg, CNRS, IPHC UMR 7178, Strasbourg, F-67000, France
[g] Department of Physics, University of Milan, Milan, I-20133, Italy
[h] Ruđer Boskovic Institute, Zagreb, HR-10002, Croatia
[i] Departamento de Ingeniería Electrónica, Universitat de Valencia, Burjassot, Valencia, Spain
[j] Grand Accélérateur National d'Ions Lourds – GANIL, CEA/DRF and CNRS/IN2P3, BP 55027, CAEN Cedex 05, F-14076, France
[k] Heavy Ion Laboratory, University of Warsaw, Warsaw, P-02-093, Poland
[l] Instituto de Física Corpuscular, CSIC-Universidad de Valencia, Valencia, E-46980, Spain
[m] Univ Lyon, Univ Claude Bernard Lyon 1, CNRS/IN2P3, IP2I Lyon, UMR 5822, Villeurbanne, F-69622, France
[n] Dipartimento di Fisica e Scienze della Terra, University of Ferrara, Ferrara, I-44122, Italy
[o] Institute for Nuclear Research, Atomki, P.O. Box 51, Debrecen, 4001, Hungary
[p] STFC Daresbury Laboratory, Daresbury, Warrington, WA4 4AD, UK
[q] INFN, Section of Florence, Florence, I-50019, Italy
[r] Department of Physics and Astronomy, Uppsala University, Uppsala, SE-75120, Sweden
[s] School of Mathematics and Physics, Faculty of Engineering and Physical Sciences, University of Surrey, Guildford, GU2 7XH, UK
[t] Institut für Kernphysik, Universität zu Köln, Köln, D-50937, Germany
[u] INFN, Section of Florence, Florence, I-50019, Italy
[v] Irfu, CEA, Université Paris-Saclay, Gif-sur-Yvette, F-91191, France

* Corresponding author.
E-mail address: Alberto.Stefanini@lnl.infn.it (A.M. Stefanini).
[1] deceased

https://doi.org/10.1016/j.physletb.2025.140084
Received 22 August 2025; Received in revised form 1 December 2025; Accepted 2 December 2025
Available online 8 December 2025

[w] Jozef Stefan Institute, Ljubljana, 1000, Slovenia
[x] GSI Helmholtzzentrum für Schwerionenforschung GmbH, Darmstadt, D-64291, Germany
[y] KTH - Royal Institute of Technology, Stockolm, SE-10044, Sweden

ARTICLE INFO

Editor: Prof. Betram Blank

Keywords:
Heavy-ion fusion
Sub-barrier cross sections
Coupled-channels model
Fusion hindrance

ABSTRACT

The sub-barrier fusion hindrance phenomenon is systematically observed in heavy-ion systems, but its evidence for light-mass cases of astrophysical interest, like C+C, C+O and O+O, is controversial. Their low-energy behaviour may be clarified by studying slightly heavier systems, so to extrapolate their trend to the lighter cases. In this work, fusion of ^{12}C + ^{28}Si has been measured down to deep sub-barrier energies, using ^{28}Si beams from the XTU Tandem accelerator of LNL on thin ^{12}C targets. Two different set-ups were employed: 1) the fusion-evaporation residues were identified by a detector telescope following an electrostatic beam separator, and 2) coincidences between the γ-ray array AGATA and segmented silicon detectors DSSD were performed, where the evaporated light charged particles were identified by pulse shape analysis. Fusion cross sections have been obtained in the wide range $\sigma \approx$150 mb – 42 nb. Coupled-channel (CC) calculations using a Woods-Saxon potential reproduce the data above $\simeq$0.1 mb. Below that, hindrance shows up and the CC results overestimate the cross sections which get close to the one-dimensional potential tunnelling limit. This suggests that the coupling strengths gradually vanish, as predicted by the adiabatic model. The hindrance threshold follows a recently updated phenomenological systematics.

1. Introduction

The phenomenon of low-energy hindrance in heavy-ion fusion is a topic of ongoing experimental and theoretical interest. It was first observed for the system ^{60}Ni + ^{89}Y [1], and it is experimentally recognised by the increasing logarithmic slope of the excitation function (or by a maximum of the S-factor) showing up at low energies.

From the theoretical point of view, extending the standard coupled-channels (CC) model to describe the hindrance effect is a theoretical challenge [2–5]. A few years ago, Simenel et al. [6,7] pointed out that the Pauli exclusion principle hinders the overlap of the two colliding nuclei, thereby influencing the ion-ion potential. As a consequence, the Coulomb barrier turns out to be thicker and higher, and low-energy fusion hindrance is produced.

For medium-mass systems, where the fusion Q-value is negative, hindrance has been systematically observed at various cross-section levels and dummyTXdummy– with different features. Representative cases are ^{64}Ni + ^{64}Ni [8], ^{16}O + ^{208}Pb [9] and ^{58}Ni + ^{54}Fe [10]. In the case of light systems, the S-factor maximum becomes broader and the hindrance threshold is more difficult to recognise. Such light systems have positive fusion Q-value, implying that the existence of an S-factor maximum is not algebraically necessary [8]. Indeed, the fusion hindrance is neither well-established nor understood in those cases. This creates uncertainties when extrapolating their trend to astrophysical energies, where it may influence the reaction rates in stellar environments [11–13].

In more detail, ^{12}C + ^{16}O [14] and ^{12}C + ^{12}C (see [15,16] and Refs. therein), the existence and the features of that phenomenon are obscured by the presence of several low-energy oscillations of the S-factor [17–21]. The case of ^{12}C + ^{13}C [22] is completely different because no oscillations and no hindrance have been observed. As the energy decreases, the S-factor tends to develop a maximum; however, it then increases again.

In this respect, we point out that recent theoretical studies [23,24] indicate the absence of the hindrance effect in both ^{12}C + ^{12,13}C. Uzawa and Hagino propose a modified fitting procedure in the low-energy range, and show that the resulting astrophysical S-factors do not show any hindrance within the range of error bars for both systems.

Because of these various features, it was proposed to study slightly heavier systems [25], to provide a reliable starting point for the extrapolation to lighter ones in the expected energy range of hindrance. We recently investigated the cases ^{12}C + ^{24,26}Mg [26,27] and ^{12}C + ^{30}Si [28]. It was observed that the hindrance energy thresholds for these systems follow the empirical estimate of Ref. [29], updated from the original formulation on the basis of those recent results and the newly published ones on ^{16}O + ^{48}Ca [30]. Moreover, the cross sections for ^{12}C + ^{24}Mg, ^{30}Si seem to approach the one-dimensional potential tunnelling limit at the lowest measured energies.

The hindrance threshold for ^{12}C + ^{24}Mg corresponds to the rather large fusion cross section ~0.9 mb, however, the experimental uncertainties are large and make that identification somewhat doubtful for this system.

In this work, we present the results of the detailed experimental study of ^{12}C + ^{28}Si, whose purpose has been to identify the hindrance phenomenon (if any), and to determine the fusion behaviour below the hindrance threshold down to far sub-barrier energies, trying to clarify as well the possible influence on hindrance of the well-known oblate deformation of ^{28}Si, in contrast with the prolate shape of ^{24,26}Mg and the spherical structure of ^{30}Si (see Ref. [31]). This information will be essential for recognising how adequate the extrapolation of the trend is to astrophysically relevant cases, on the basis of measured cross-sections at very low energies. Previous fusion data on ^{12}C + ^{28}Si are available only well above the barrier [32–36].

We have used two different and complementary setups to investigate the fusion excitation function of ^{12}C + ^{28}Si down to cross sections as small as $\approx$40 nb. The measurements were performed at Laboratori Nazionali di Legnaro (LNL) of INFN, using the electrostatic deflector setup [10] for the high-energy part, and the AGATA γ-ray spectrometer [37] associated with segmented silicon detectors (DSSD) for the identification of evaporated light charged particles, at the lower energies.

Sect. II describes the experimental set-ups and methods of data analysis, and shows the results that are then compared in Sect. III with CC calculations. Systematic trends are discussed in Section IV comparing with near-by systems and concerning the astrophysical aspects of the results as well. Section V presents the conclusions of the present work.

2. Experimental set-ups

The ^{28}Si beams of the XTU Tandem at LNL were employed, with currents 15–30 pnA, in the energy range 29.5–54 MeV. Thin ^{12}C targets ~50 $\mu g/cm^2$ were used, with isotopic enrichment of 99.8%, to minimise the beam energy corrections and straggling effects that may increase the unwanted background. In the measurements with the electrostatic separator set-up of LNL, the evaporation residues (ER) were detected using a $\Delta E - E$ gas-silicon detector and large position-sensitive micro-channel plates (MCP) detectors. Two time of flights (ToF) were measured between the silicon detector and the two MCP.

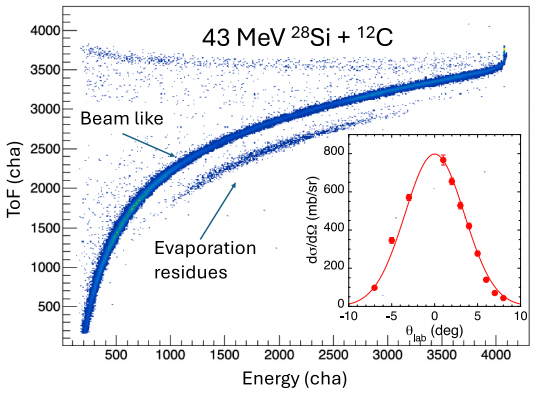

Fig. 1. Two-dimensional spectrum Time-of-Flight vs Energy measured at E_{lab} = 43 MeV and $\theta_{lab} = 3°$. The group of evaporation residue (ER) events is indicated, well separated from beam-like ions. The insert shows the angular distribution of ER, together with the Gaussian fit, at the same energy.

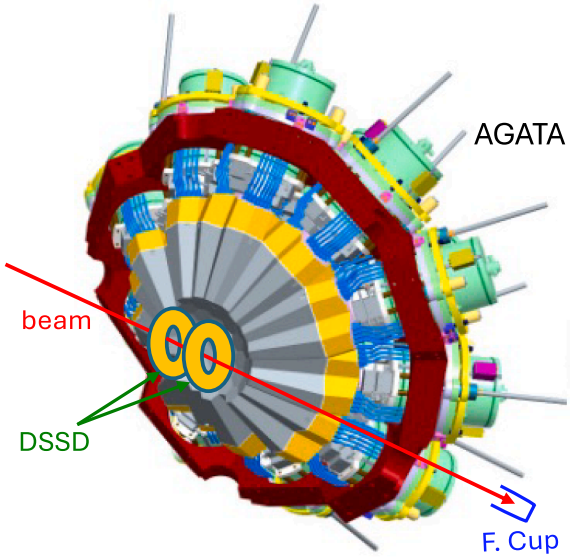

Fig. 2. Schematic view of the setup used for the AGATA-DSSD measurements. The target (not shown in the figure) is placed between the two DSSD.

The beam control and yield normalisation to the Rutherford cross section were ensured by four silicon detectors placed at $\theta_{lab} = 16°$ in the scattering chamber (see Ref. [10] for further details).

The ER angular distribution was measured at E_{lab} = 43 MeV in the θ_{lab} range from -7° to +8°, and it is reported in Fig. 1. It is well fitted by a single Gaussian curve (red line), and it allowed us to extrapolate its shape to the other energies where the fusion yield was measured at only $\theta_{lab} = 2°$ (or 3° at low energies). The fusion cross section was obtained by integrating that distribution. Standard PACE4 calculations [38] anticipate that the shape of the angular distribution does not appreciably vary with energy in the measured range. This has been validated by several previous measurements (see e.g. Refs. [28,39]). The systematic error on the cross-section scale is estimated to be ±7-8% as in previous experiments with that setup [10].

Following the technique introduced by Jiang et al. [40], we extended the fusion excitation function down to very small cross sections, using the γ-ray tracking spectrometer AGATA [37] and two annular Double Sided Silicon strip Detectors (DSSD) (4" diameter) placed 5 cm upstream and downstream of the target (see Fig. 2). Their thicknesses were 0.5 and 1.5 mm, respectively, covering the angular ranges θ_{lab} = 139.6°–162.7° and 23.0°–40.4°, and have been used to detect coincident events between

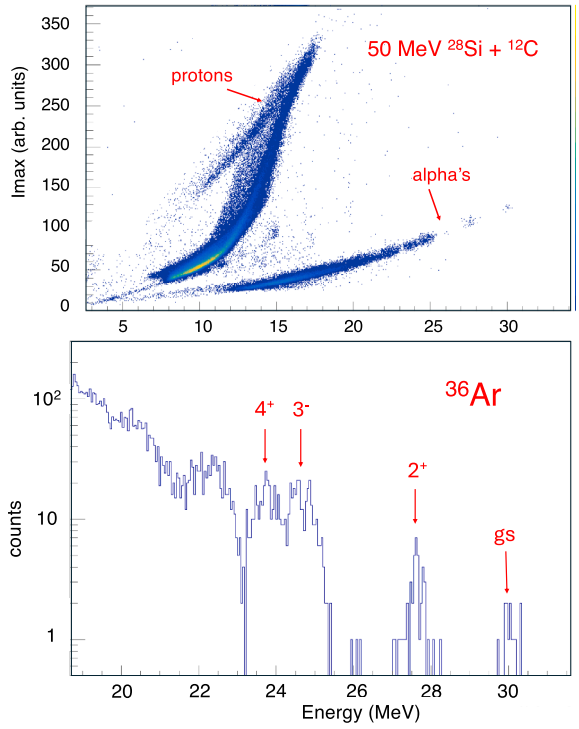

Fig. 3. (top panel) Events detected in an intermediate ring ($\theta \simeq 29°$) of the forward DSSD. Protons and α particles are identified through pulse shape analysis (*psa*), plotting the maximum of the signal derivative (I_{max}) vs their energy E. (bottom panel) Energy spectrum of the corresponding α particles. Several particle groups populating different states in the ^{36}Ar residual nucleus can be observed.

the evaporated light charged particles and the prompt γ-rays emitted from the various residual nuclei (see Fig. 2 of Ref. [41]).

The measurements were performed at four ^{28}Si beam energies with this setup, i.e., E_{lab} = 50, 34 MeV, to overlap with points taken with the electrostatic deflector, and at the very low energies of 31 and 29.5 MeV. Nickel absorbers of calibrated thickness were placed in front of the two DSSD (15μm for the forward one, and 2μm for the backward one) to stop the scattered beam, target recoils, and the electrons coming from the target. Particle identification by pulse shape analysis was made possible by installing both DSSD with the ohmic side facing the target [42]. Fig. 3 (top panel) shows the good separation obtained between evaporated protons and α-particles down to rather low energies. The direct population of states in the exit channels can then be observed, fixing an emission angle, by projecting this matrix onto the energy axis. This is shown in the bottom panel of Fig. 3, for the α-particles selected in the top matrix.

The energy of the evaporated particle, when associated with its emission angle, yields the total excitation of the system. By correlating this excitation energy with the γ-ray energy, one can identify the events belonging to a certain evaporation channel. Fig. 4 shows, as a representative example, this correlation matrix obtained at E_{lab} = 50 MeV, where all events detected by the two DSSD have been considered (top panel). The bottom panel is the projection on the E_γ axis, where one can recognise the γ-lines marked in the matrix.

This representation is useful even at very low energies, as shown in Fig. 5 for E_{lab} = 31 MeV, where the eight fusion events populating ^{38}Ar by 2p evaporation (corresponding to a cross section of ≃200 nb) are very cleanly identified.

For each experimental run/energy, the ER level schemes provided us with the number of γ-particle coincidence events associated with each γ transition feeding the corresponding ground states. Electron conversion might compete with gamma decay; however, it brings a very small

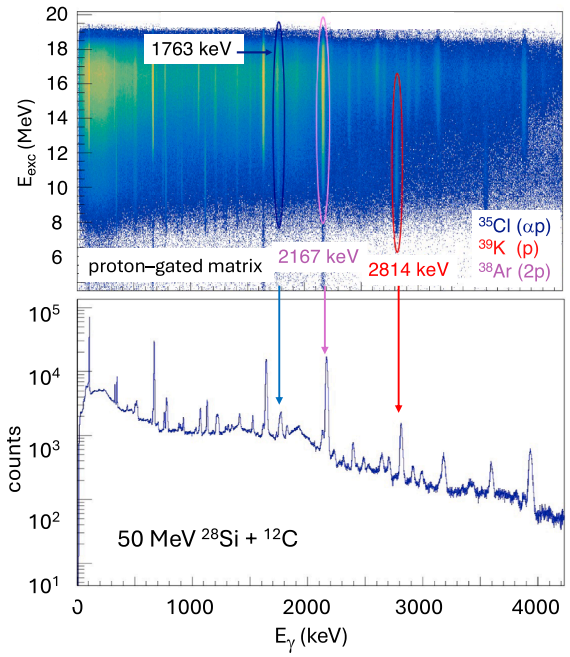

Fig. 4. (top panel) Two-dimensional excitation energy vs Doppler-corrected γ-ray energy spectrum for proton events at $E_{lab} = 50$ MeV. (bottom panel) Projection of the matrix onto the E_γ axis.

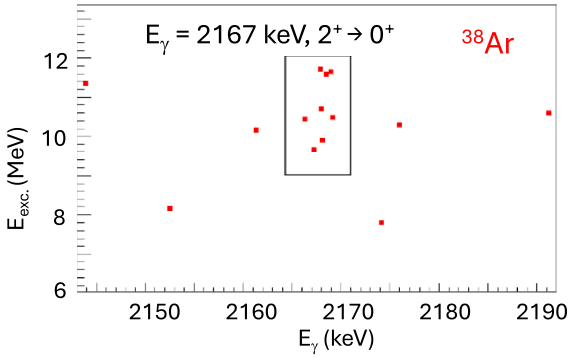

Fig. 5. Zoomed matrix for the 2p evaporation channel ^{38}Ar excitation energy (E_{exc}) vs γ-ray energy at $E_{lab} = 31$ MeV, where the few fusion events are clearly identified. The total fusion cross section at this energy, including the other observed evaporation channel (1α) is $(3.0\pm1.1)\ 10^{-4}$ mb, please see Table 1.

contribution (a few per thousand) to those transitions [43] in the mass region A~36-40.

The normalisation between different runs was ensured by two 50 mm^2 silicon monitor detectors, installed at $\theta_{lab} = 12°$ at around 50 cm from the target. Finally, the absolute cross section scale was fixed, taking as reference the energy point at $E_{lab} = 50$ MeV that was measured also using the electrostatic deflector set-up, whose absolute efficiency is well known for the present system (and several others). Normalising this way the excitation function to the electrostatic deflector results, takes into account also the possible contribution of pure neutron evaporation channels that are not obviously observed in the AGATA-DSSD coincidences, and actually not even in the γ-ray singles spectra at any energy. Moreover, the normalization also takes into account possible effects due to the angular distribution of gamma rays since Agata does not cover all θ angles in the present configuration. We point out that the adopted normalisation, above the barrier, brings the point at $E_{lab} = 34$ MeV in very good agreement with the nearby ones obtained with the electrostatic deflector.

Table 1
Fusion cross sections of ^{12}C + ^{28}Si measured in this work via AGATA-DSSD coincidences. The data for the observed evaporation channels at each energy are specified. The quoted errors are statistical uncertainties. The upper cross section limits quoted for the $1p$ channel at the two lowest energies, correspond to the case where one coincidence event would have been clearly identified.

channel	σ (mb)
$E_{c.m.}$ (MeV) = 8.71	
(1p	<1.5 10^{-5})
2p	2.62±1.31 10^{-5}
1α	1.54±1.09 10^{-5}
Total	4.16±1.70 10^{-5}
$E_{c.m.}$ (MeV) = 9.16	
(1p	<1.5 10^{-5})
2p	1.6±0.6 10^{-4}
1α	1.4±0.9 10^{-4}
Total	3.0±1.1 10^{-4}
$E_{c.m.}$ (MeV) = 10.06	
1p	0.0054±0.0011
2p	0.0066±0.0007
1α	0.0027±0.0006
Total	0.0147±0.0015
$E_{c.m.}$ (MeV) = 14.94	
1p	17.50±0.09
2p	68.2±0.1
1p1n	6.39±0.04
1p1α	53.3±0.2
1α	7.33±0.05
1n1α	0.58±0.01
2α	4.80±0.03
Total	158±1

Subsequently, those yields were normalised using 1) the AGATA efficiency vs γ-ray energy in the used geometry, obtained by a measurement with a ^{152}Eu source, performed just after the experiment, in agreement with the simulations of Ref. [37], extending to high γ-ray energies, and 2) the DSSD detectors' efficiencies. These are determined by their angular coverage (≈26% of 4π), by kinematics and by the electronic thresholds. The sum of all such normalised yields of coincident events, plus those directly feeding the ER ground states (see e.g. Fig. 3), is then proportional to the fusion cross section measured in the considered run.

At the various energies, the evaporation channels observed in coincidence events were $1p$, $2p$, $1pn$, 1α, $1p1\alpha$, $1n1\alpha$ and 2α. Details of those channels and of the corresponding measured cross sections are listed in Table 1.

3. Coupled-channels calculations

The fusion excitation function was calculated with the CCFULL code [44] using the coupled-channels (CC) formalism employed in several heavy-ion fusion reactions analyses in recent years. CCFULL takes into account channel couplings to all orders and uses the so-called rotating frame [45] or isocentrifugal [46] approximation, which considerably reduces the number of channels, thus simplifying the calculations. A Woods-Saxon potential with parameters $V_o = 44.6$ MeV, $r_o = 1.06$ fm and $a = 0.61$ fm was used to fit the experimental data near the barrier.

In the calculation, ^{12}C was considered inert, while the lowest quadrupole and octupole excitations of ^{28}Si were included, with the adopted deformation parameters $\beta_2 = -0.41$ [47] and $\beta_3 = 0.40$ [48], respectively. The quadrupole deformation parameter of ^{28}Si is negative,

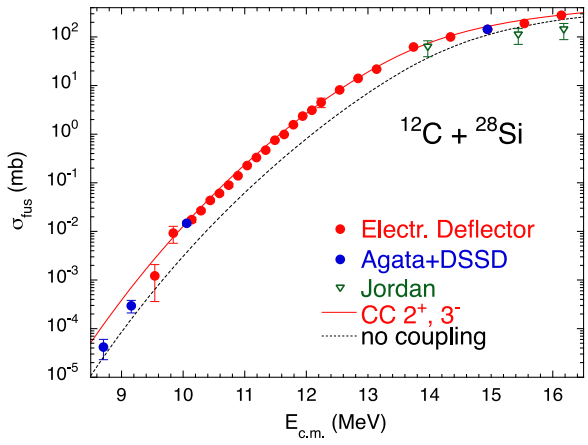

Fig. 6. Measured excitation function of ^{12}C + ^{28}Si, compared to CC calculations. The red dots are the points measured with the electrostatic deflector set-up. The blue dots refer to the measurements performed the AGATA + DSSD combination. The triangles report the results of Jordan et al. [32]. See text for more details.

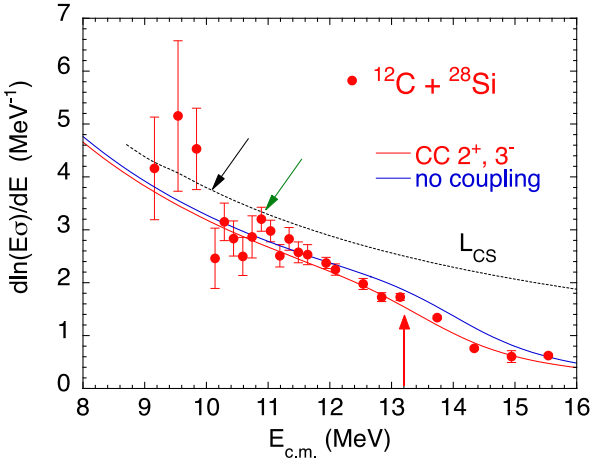

Fig. 7. The logarithmic derivative of the energy-weighted excitation function for ^{12}C + ^{28}Si, compared with the results of CC and no-coupling calculations. The L_{CS} line represents the slope expected for a constant S-factor, for each energy.

since this nucleus is oblate [31]. The mutual excitation of both 2^+ and 3^- states was neglected because of its very high excitation energy.

We show in Fig. 6 the obtained excitation function, where the quoted errors are only statistical uncertainties, together with the results of CC calculations. The lowest energy points previously obtained by Jordan et al. [32] are also reported. One sees that the energy overlap between the present and previous data set is marginal, and that a reasonable agreement is observed, although Jordan's data appear to be flatter vs energy. The present experimental cross sections are well reproduced by the calculation down to ≈10 MeV. Below this energy, we have clear evidence of the hindrance phenomenon, and that the three lowest energy points approach and appear to follow the trend of the no-coupling limit.

To be noted that the low-energy behaviour of ^{12}C + ^{28}Si has been evidenced, even if the experimental uncertainties are rather large, only thanks to the measurements performed with the AGATA spectrometer.

Fig. 7 shows the logarithmic derivative (slope) of the excitation function obtained from the measured cross sections, as the incremental ratio of two near-by points. The slope increases with decreasing energy and touches the L_{CS} line at around 11 MeV (green arrow). A decrease is then observed, followed by a pronounced crossing at ≃10.1 MeV (black arrow). This is the energy that we can associate to the hindrance threshold in ^{12}C + ^{28}Si.

In the same figure, we report the results of the CC calculations and the no-coupling limit. The theoretical curves yield a flat trend for the slope in the plotted energy range, as actually expected. They are close to each other, as a consequence of the rather high energies of the ^{28}Si coupled excitations. The experimental trend is well reproduced by the calculations; however, not where hindrance shows up (and possibly around 11 MeV). This is expected, since one knows that a potential of WS shape is not able, in general, to fit cross sections in the hindrance region [2].

4. Comparison with nearby systems

We refer to Fig. 8, where the abscissa is the energy with respect to the Coulomb barrier produced by the Akyüz-Winther (AW) potential [49]. We note the similarity between the logarithmic derivatives of the three systems shown there. With decreasing energy, the three cases exhibit small oscillations followed by a larger slope increase that we associate with the onset of hindrance, at similar E/V_b values. This is an indication that the different structure of ^{28,30}Si and ^{26}Mg has a minor influence on the hindrance threshold.

^{12}C + ^{24}Mg [26] (not shown here), has an analogous trend, as Fig. 4 of Ref. [27] clearly shows, but with larger experimental uncertainties.

In all cases, besides the occurrence of hindrance, smaller slope oscillations are systematically observed, whose origin still lacks a realistic explanation.

The analogy between the behaviour of ^{12}C + ^{28}Si and other nearby cases at low energy can be appreciated in Fig. 9, where the ratio of the measured cross section to the calculated one in the no-coupling limit is plotted vs the energy difference from the barrier. This representation was already used in Ref. [26]. One sees that fusion enhancement is larger for the relatively heavier ^{48}Ca + ^{48}Ca [50], as expected because the coupling strengths scale with the factor $Z_1 Z_2$. This more than compensates the stiff structure of ^{48}Ca. Therefore, the ratio $\sigma_{exp}/\sigma_{noc}$ could not be observed below a certain limit for this system. For ^{16}O + ^{48}Ca, the enhancement is rather small, very similar to the systems ^{12}C + ^{24}Mg, ^{30}Si. This is due to the limited effect of the channel couplings, given the doubly magic nature of the two nuclei.

The present case ^{12}C + ^{28}Si has an enhancement larger than the other systems cited here above. In particular, the enhancement observed for ^{12}C + ^{28}Si is larger than for ^{12}C + ^{30}Si. This is due to the deformed (oblate) character of ^{28}Si while ^{30}Si is spherical. Also, the lowest 2^+ excitation is lower and stronger in the ^{28}Si case [47].

The very small cross sections that have been measured for ^{12}C + ^{28}Si allow showing that the enhancement ratio reduces to one at the lowest

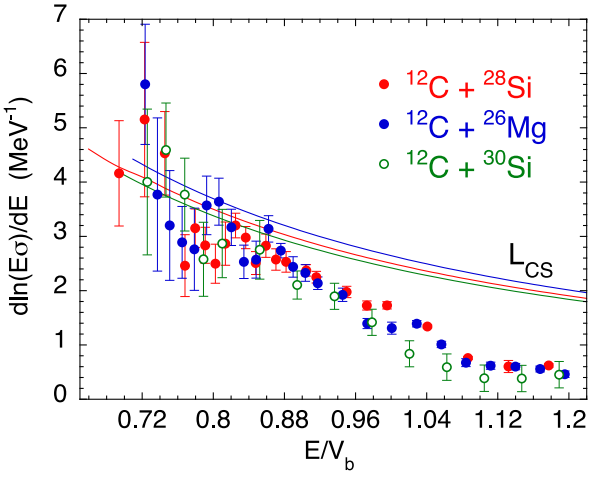

Fig. 8. Logarithmic derivatives of the energy-weighted excitation functions for ^{12}C + ^{28}Si (in red), ^{12}C + ^{26}Mg (blue dots) [27] and ^{12}C + ^{30}Si (open green dots). The three L_{CS} lines are close to each other.

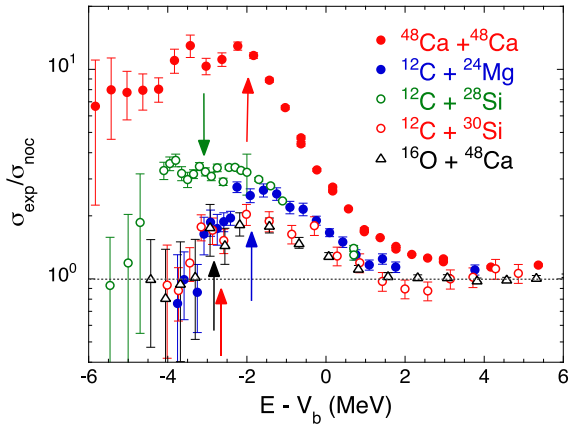

Fig. 9. Ratio of the experimental fusion cross sections to the results of no-coupling calculations vs the energy difference from the Coulomb barrier, for the four indicated systems [28,30,50], and for ^{12}C + ^{28}Si. The vertical arrows mark the hindrance threshold for the different cases (see also Ref. [51]). The thresholds for ^{12}C + ^{28,30}Si are very close to each other (10.1 MeV and 10.45MeV, respectively).

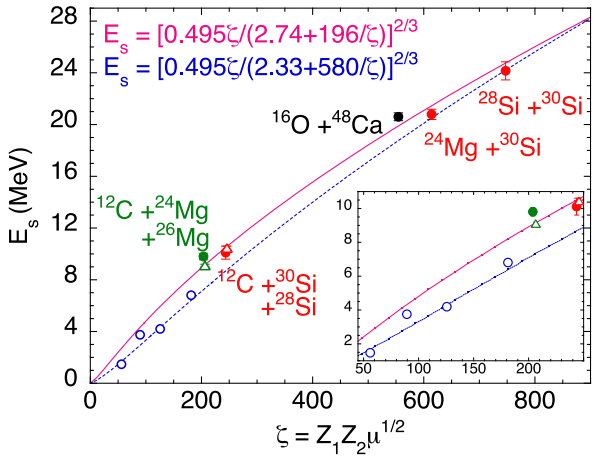

Fig. 10. Threshold energies for hindrance in light systems, including the present case ^{12}C + ^{28}Si. The uncertainties are smaller than the symbol size for some of the reported points. The insert is a zoom of the figure on the lighter systems (see text for further details).

energies (even if errors are rather large). The trend at even lower energies is unknown, and the question is: do the cross-sections follow the no-coupling limit or go below that, taking into account that the significance of a two-body potential becomes questionable at the very low energies where the ion-ion distances are smaller than the touching point? This is an interesting issue that warrants further investigation.

Fig. 10 reports the systematics of the fusion hindrance threshold for light and medium-light systems as recently presented in Ref. [30]. The open blue symbols represent, with increasing system parameter ζ, ^{10}B + ^{10}B, ^{12}C + ^{12}C, ^{12}C + ^{16}O and ^{16}O + ^{16}O, which were obtained by extrapolating the corresponding data from higher energies using the hindrance model [51] (no error bars were quoted for these points in that work).

Indeed, this kind of representation was originally developed by Jiang et al. [29] for heavier stiff systems, even if the light systems of astrophysical relevance were included in the fit (blue dashed line). No particular importance was attributed to the mass symmetry of the system. Obviously, the present case ^{12}C + ^{28}Si and the near-by ones ^{12}C + ^{30}Si, ^{24,26}Mg had not yet been measured, as well as ^{16}O + ^{48}Ca. These systems have been included in the updated fit of Ref. [30] (solid red line), that well reproduces heavier systems with ζ values outside the range of the Figure.

On the other side, the new fit does not include the astrophysical systems and the result differs from the previous one, in particular for those light cases, predicting for them a higher hindrance threshold. This is a direct consequence of the behaviour of the medium-light systems established in recent years (including the present case ^{12}C + ^{28}Si), which places on more solid grounds the extrapolation into the region of the light astrophysical systems at very low energies.

The higher fitted hindrance threshold in that mass region may appear a minimal variation, but it may lead to significant changes in the value of the S-factors/reaction rates. This is especially true for reactions occurring in the late evolution of massive stars and in type-Ia supernovae [52], modifying the nucleosynthesis processes and thus the abundance of many isotopes. The specific consequences of those reduced astrophysical reaction rates depend on the details of the stellar environment and go beyond the scope of the present work.

5. Summary

We have presented the results of the experimental study of fusion near and below the barrier of the heavy-ion system ^{12}C + ^{28}Si. The measurements were performed at LNL 1) by the electrostatic beam deflector set-up and 2) by the γ-ray tracking spectrometer AGATA [37] in coincidence with two annular DSSD detecting the light charged particles evaporated from the compound nucleus ^{40}Ca. The combination of the two methods allowed us to measure a wide range of fusion cross sections from above the barrier down to very small values ≈42 nb. We note that, for the first time, the integration of two complementary setups has been applied to fusion studies far below the barrier.

Particle identification was performed by pulse shape discrimination in the DSSD [42]. The direct population of states in the exit channels could be observed in the energy spectrum of the evaporated particles (α's and protons), by selecting an emission θ angle. Several groups of particles are observed with good energy resolution.

CC calculations using a WS potential are able to reproduce the cross sections down to about E_{cm}≃10.1 MeV, corresponding to σ ≃15 μb, where the hindrance phenomenon shows up. This is also clearly indicated by the trend of the logarithmic derivative of the excitation function. The behaviour of nearby systems, as far as that slope is concerned, is quite similar.

This similarity also shows up for the trend of the excitation functions at very low energies, that is, the cross sections are consistent with the simple tunnelling of a one-dimensional potential barrier. This behaviour is beyond doubt for the present case ^{12}C + ^{28}Si. Whether, at still smaller energies, the cross sections follow the no-coupling limit or turn out to be even lower should be clarified by further experimental investigations.

Significant consequences may follow for the lighter systems relevant for astrophysics. Indeed, the hindrance effect in those cases would reduce the reaction rate of carbon and oxygen burning in the astrophysical environments.

Data availability

Data will be made available on request.

Declaration of competing interests

The authors declare that they have no known competing financial interests or personal relationships that could have appeared to influence the work reported in this paper.

Acknowledgements

We acknowledge the high-quality work of the XTU Tandem staff and M. Loriggiola for preparing the targets of excellent quality. The research leading to the present results has received funding from

the European Union's Horizon 2020 research and innovation programme under grant agreement No 654002. Work partially funded by MCIN/AEI/10.13039/501100011033, Spain with grants PID2020-118265GB-C4, PID2023-150056NB-C4, PRTR-C17.I01, by Generalitat Valenciana, Spain, with grant CIPROM/2022/54, ASFAE/2022/031 and by the EU NextGenerationEU and FEDER funds.

References

[1] C.L. Jiang, H. Esbensen, K.E. Rehm, B.B. Back, R. Janssens, J.A. Caggiano, P. Collon, J. Greene, A.M. Heinz, D.J. Henderson, I. Nishinaka, T.O. Pennington, D. Seweryniak, Unexpected behavior of heavy-ion fusion cross sections at extreme sub-barrier energies, Phys. Rev. Lett. 89 (2002) 052701. https://doi.org/10.1103/PhysRevLett.89.052701

[2] S. Misicu, H. Esbensen, Signature of shallow potentials in deep sub-barrier fusion reactions, Phys. Rev. C 75 (2007) 034606. https://doi.org/10.1103/PhysRevC.75.034606

[3] H. Esbensen, S. Misicu, Hindrance of ^{16}O + ^{208}Pb fusion at extreme sub-barrier energies, Phys. Rev. C 76 (2007) 054609. https://doi.org/10.1103/PhysRevC.76.054609

[4] T. Ichikawa, K. Hagino, A. Iwamoto, Existence of a one-body barrier revealed in deep subbarrier fusion, Phys. Rev. C 75 (2007) 057603. https://doi.org/10.1103/PhysRevC.75.057603

[5] T. Ichikawa, Systematic investigations of deep sub-barrier fusion reactions using an adiabatic approach, Phys. Rev. C 92 (2015) 064604. https://doi.org/10.1103/PhysRevC.92.064604

[6] C. Simenel, A.S. Umar, K. Godbey, M. Dasgupta, D.J. Hinde, How the Pauli exclusion principle affects fusion of atomic nuclei, Phys. Rev. C 95 (2017) 031601. https://doi.org/10.1103/PhysRevC.95.031601

[7] C. Simenel, Nuclear quantum many-body dynamics (2nd edition)-From collective vibrations to heavy-ion collisions, Eur. Phys. J. A 61 (7) (2025) 181. https://doi.org/10.1140/epja/s10050-025-01624-3

[8] C.L. Jiang, B.B. Back, H. Esbensen, R.V.F. Janssens, K.E. Rehm, Systematics of heavy-ion fusion hindrance at extreme sub-barrier energies, Phys. Rev. C 73 (2006) 014613. https://doi.org/10.1103/PhysRevC.73.014613

[9] M. Dasgupta, D.J. Hinde, A. Diaz-Torres, B. Bouriquet, C.I. Low, G.J. Milburn, J.O. Newton, Beyond the coherent coupled channels description of nuclear fusion, Phys. Rev. Lett. 99 (19) (2007) 192701. https://doi.org/10.1103/PhysRevLett.99.192701

[10] A.M. Stefanini, G. Montagnoli, L. Corradi, S. Courtin, E. Fioretto, A. Goasduff, F. Haas, P. Mason, R. Silvestri, P.P. Singh, F. Scarlassara, S. Szilner, Fusion hindrance for ^{58}Ni + ^{54}Fe, Phys. Rev. C 82 (2010) 014614. https://doi.org/10.1103/PhysRevC.82.014614

[11] L.R. Gasques, E.F. Brown, A. Chieffi, C.L. Jiang, M. Limongi, C. Rolfs, M. Wiescher, D.G. Yakovlev, Implications of low-energy fusion hindrance on stellar burning and nucleosynthesis, Phys. Rev. C 76 (2007) 035802. https://doi.org/10.1103/PhysRevC.76.035802

[12] T. Dumont, E. Monpribat, S. Courtin, A. Choplin, A. Bonhomme, S. Ekström, M. Heine, D. Curien, J. Nippert, G. Meynet, Massive star evolution with a new 12C + 12C nuclear reaction rate - The core carbon-burning phase, A&A, 688, (2024).

[13] T. Dumont, A. Bonhomme, A. Griffiths, A. Choplin, M.A. Aloy, G. Meynet, K. Godbey, C. Simenel, G. Scamps, F. Castillo, A. Cosoli-Ortega, S. Courtin, The advanced evolution of massive stars: I. new reaction rates for carbon and oxygen nuclear reactions, Astron. Astrophys. 702 (2025) A86. https://doi.org/10.1051/0004-6361/202555326

[14] X. Fang, W.P. Tan, M. Beard, R.J. de Boer, G. Gilardy, H. Jung, Q. Liu, S. Lyons, D. Robertson, K. Setoodehnia, C. Seymour, E. Stech, B. Van de Kolk, M. Wiescher, R.T. de Souza, S. Hudan, V. Singh, X.D. Tang, E. Uberseder, Experimental measurement of ^{12}C + ^{16}O fusion at stellar energies, Phys. Rev. C 96 (2017) 045804. https://doi.org/10.1103/PhysRevC.96.045804

[15] W.P. Tan, A. Boeltzig, C. Dulal, R.J. de Boer, B. Frentz, S. Henderson, K.B. Howard, R. Kelmar, J.J. Kolata, J. Long, K.T. Macon, S. Moylan, G.F. Peaslee, M. Renaud, C. Seymour, G. Seymour, B. Van de Kolk, M. Wiescher, E.F. Aguilera, P. Amador-Valenzuela, D. Lizcano, E. Martinez-Quiroz, New measurement of ^{12}C + ^{12}C fusion reaction at astrophysical energies, Phys. Rev. Lett. 124 (2020) 192702. https://doi.org/10.1103/PhysRevLett.124.192702

[16] G. Fruet, S. Courtin, M. Heine, D.G. Jenkins, P. Adsley, A. Brown, R. Canavan, W.N. Catford, E. Charon, D. Curien, S. Della Negra, J. Duprat, F. Hammache, J. Lesrel, G. Lotay, A. Meyer, D. Montanari, L. Morris, M. Moukaddam, J. Nippert, Z. Podolyak, P.H. Regan, I. Ribaud, M. Richer, M. Rudigier, R. Shearman, N. de Sereville, C. Stodel, Advances in the direct study of carbon burning in massive stars, Phys. Rev. Lett. 124 (2020) 192701. https://doi.org/10.1103/PhysRevLett.124.192701

[17] D. A. Bromley, J. A. Kúhner, E. Almqvist, Resonant elastic scattering of ^{12}C by carbon, Phys. Rev. Lett., 4 (1960), 365, https://doi.org/10.1103/PhysRevLett.4.365.

[18] K. A. Erb, R. R. Betts, S. K. Korotky, M. M. Hindi, P. P. Tung, M. W. Sachs, S. J. Willett, D. A. Bromley, Resonant elastic scattering of ^{12}C by carbon, Phys. Rev. C, 22, (1980), 507, https://doi.org/10.1103/PhysRevC.22.507.

[19] M. Freer, H. Horiuchi, Y. Kanada-En'yo, D. Lee, U.-G. Meißner, Microscopic clustering in light nuclei, Rev. Mod. Phys. 90 (2018) 035004. https://doi.org/10.1103/RevModPhys.90.035004

[20] A. Diaz-Torres, M. Wiescher, Characterizing the astrophysical S factor for ^{12}C + ^{12}C fusion with wave-packet dynamics, Phys. Rev. C 97 (2018) 055802. https://doi.org/10.1103/PhysRevC.97.055802

[21] C.L. Jiang, B.B. Back, H. Esbensen, R.V.F. Janssens, K.E. Rehm, R.J. Charity, Origin and consequences of ^{12}C + ^{12}C fusion resonances at deep sub-barrier energies, Phys. Rev. Lett. 110 (2013) 072701. https://doi.org/10.1103/PhysRevLett.110.072701

[22] N.T. Zhang, X.Y. Wang, D. Tudor, B. Bucher, I. Burducea, H. Chen, Z.J. Chen, D. Chesneanu, A.I. Chilug, L.R. Gasques, D.G. Ghita, C. Gomoiu, K. Hagino, S. Kubono, Y.J. Li, C.J. Lin, W.P. Lin, R. Margineanu, A. Pantelica, I.C. Stefanescu, M. Straticiuc, X.D. Tang, L. Trache, A.S. Umar, W.Y. Xin, S.W. Xu, Y. Xu, Constraining the ^{12}C + ^{12}C astrophysical S-factors with the ^{12}C + ^{13}C measurements at very low energies, Phys. Lett. B 801 (2020) 135170. https://doi.org/10.1016/j.physletb.2019.135170

[23] K. Godbey, C. Simenel, A.S. Umar, Absence of hindrance in a microscopic ^{12}C + ^{12} C fusion study, Phys. Rev. C 100 (2019) 024619. https://doi.org/10.1103/PhysRevC.100.024619

[24] K. Uzawa, K. Hagino, Re-examination of fusion hindrance in astrophysical ^{12}C + ^{12}C and ^{12}C + ^{13}C reactions, 2025. arXiv:2507.18065

[25] C.L. Jiang, A.M. Stefanini, H. Esbensen, K.E. Rehm, S. Almaraz-Calderon, B.B. Back, L. Corradi, E. Fioretto, G. Montagnoli, F. Scarlassara, D. Montanari, S. Courtin, D. Bourgin, F. Haas, A. Goasduff, S. Szilner, T. Mijatovic, Fusion hindrance for a positive Q-value system ^{24}Mg + ^{30}Si, Phys. Rev. Lett. 113 (2014) 022701. https://doi.org/10.1103/PhysRevLett.113.022701

[26] G. Montagnoli, A.M. Stefanini, C.L. Jiang, K. Hagino, F. Niola, D. Brugnara, P. Colovic, G. Colucci, L. Corradi, R. Depalo, E. Fioretto, A. Goasduff, G. Pasqualato, F. Scarlassara, S. Szilner, I. Zanon, Fusion of ^{12}C + ^{24}Mg at extreme sub-barrier energies, J.Phys. G 49 (2022) 095101. https://doi.org/10.1088/1361-6471/ac7edd

[27] A.M. Stefanini, G. Montagnoli, M. Del Fabbro, D. Brugnara, G. Colucci, L. Corradi, J. Diklic, E. Fioretto, F. Galtarossa, A. Goasduff, M. Mazzocco, J. Pellumaj, E. Pilotto, L. Zago, I. Zanon, Sub-barrier fusion in ^{12}C + ^{26,24}Mg: hindrance and oscillations, Phys. Rev. C 108 (2023) 014602. https://doi.org/10.1103/PhysRevC.108.014602

[28] G. Montagnoli, A.M. Stefanini, C.L. Jiang, K. Hagino, F. Galtarossa, G. Colucci, S. Bottoni, C. Broggini, A. Caciolli, P. Colovic, L. Corradi, S. Courtin, R. Depalo, E. Fioretto, G. Fruet, A. Gal, A. Goasduff, M. Heine, S.P. Hu, M. Kaur, T. Mijatovic, M. Mazzocco, D. Montanari, F. Scarlassara, E. Strano, S. Szilner, G.X. Zhang, Fusion hindrance for the positive Q-value system ^{12}C + ^{30}Si, Phys. Rev. C 97 (2018) 024610. https://doi.org/10.1103/PhysRevC.97.024610

[29] C.L. Jiang, K.E. Rehm, B.B. Back, R.V.F. Janssens, Survey of heavy-ion fusion hindrance for lighter systems, Phys. Rev. C 79 (2009) 044601. https://doi.org/10.1103/PhysRevC.79.044601

[30] A.M. Stefanini, G. Montagnoli, M. Del Fabbro, F. Fontana, P. Aguilera, G. Andreetta, D. Brugnara, G. Colucci, L. Corradi, E. Fioretto, F. Galtarossa, A. Goasduff, B.G. Servin, A. Gozzelino, M. Heine, G. Harmant, D. Mengoni, M. Luciani, K. Rezynkina, S. Rocca, D. Stramaccioni, Low-energy fusion of doubly magic nuclei: the notable case of ^{16}O + ^{48} Ca, Phys. Rev. C 111 (2025) 064620. https://doi.org/10.1103/hj5x-r1gw

[31] N.J. Stone, Table of nuclear magnetic dipole and electric quadrupole moments, At. Data Nucl. Data Tables 90 (2005) 75. https://doi.org/10.1016/j.adt.2005.04.001

[32] W. J. Jordan, J. V. Maher, J. C. Peng, The fusion of ^{12}C and ^{16}O with ^{28,29,30}Si, Phys. Lett. B, 87, (1979), 38, https://doi.org/10.1016/0370-2693(79)90012-1.

[33] S. Gary, C. Volant, Fusion and compound nuclei decay for light and intermediate-mass systems: ^{24}Mg, ^{28}Si + ^{12}C, ^{24}Mg + ^{24,26}Mg, ^{28}Si + ^{24}Mg, ^{28,29,30}Si, Phys. Rev. C 25 (1982) 1877. https://doi.org/10.1103/PhysRevC.25.1877

[34] K.T. Lesko, D.-K. Lock, A. Lazzarini, R. Vandenbosch, V. Metag, H. Doubre, Energy dependence of fusion cross section for ^{28}Si + ^{12}C by evaporation residue measurements, Phys. Rev. C 25 (1982) 872. https://doi.org/10.1103/PhysRevC.25.872

[35] Y. Nagashima, S.M. Lee, M. Sato, J. Schimizu, T. Nakagawa, Y. Fukuchi, K. Furuno, M. Yamanouchi, T. Mikumo, Fusion cross section for ^{28}Si + ^{12}C, Phys. Rev. C 26 (1982) 2661. https://doi.org/10.1103/PhysRevC.26.2661

[36] B.A. Harmon, S.T. Thornton, D. Shapira, J. Gomez del Campo, M. Beckerman, Entrance channel limit on the fusion of ^{28}Si with ^{12}C at high energy, Phys. Rev. C 34 (1986) 552. https://doi.org/10.1103/PhysRevC.34.552

[37] J.J. Valiente-Dobón, R. Menegazzo, A. Goasduff, et al., Conceptual design of the AGATA 2π array at LNL, Nucl. Instr. and Meth. in Phys. Res. A 1049 (2023) 168040. https://doi.org/10.1016/j.nima.2023.168040

[38] A. Gavron, Statistical model calculations in heavy ion reactions, Phys. Rev. C 21 (1980) 230. https://doi.org/10.1103/PhysRevC.21.230

[39] G. Montagnoli, A.M. Stefanini, H. Esbensen, C.L. Jiang, L. Corradi, S. Courtin, E. Fioretto, A. Goasduff, J. Grebosz, F. Haas, M. Mazzocco, C. Michelagnoli, T. Mijatovic, D. Montanari, C. Parascandolo, K.E. Rehm, F. Scarlassara, S. Szilner, X.D. Tang, C.A. Ur, Effects of transfer channels on near- and sub-barrier fusion of ^{32}S + ^{48}Ca, Phys. Rev. C 87 (2013) 014611. https://doi.org/10.1103/PhysRevC.87.014611

[40] C.L. Jiang, K.E. Rehm, X. Fang, X.D. Tang, M. Alcorta, B.B. Back, B. Bucher, P. Collon, C.M. Deibel, B. DiGiovine, J.P. Greene, D.J. Henderson, R.V.F. Janssens, T. Lauritsen, C.J. Lister, S.T. Marley, R.C. Pardo, D. Seweryniak, C. Ugalde, S. Zhu, M. Paul, Measurements of fusion cross-sections in ^{12}C + ^{12}C at low beam energies using a particle-γ coincidence technique, Nucl. Instr. Meth. Phys. Res. A 682 (2012) 12. https://doi.org/10.1016/j.nima.2012.03.051

[41] D. Brugnara, G. Montagnoli, A.M. Stefanini, M. Del Fabbro, P.A. Aguilera Jorquera, G. Andreetta, F. Angelini, M. Balogh, J. Benito, G. Benzoni, A. Bonhomme, S. Bottoni, S. Carollo, G. Colucci, L. Corradi, S. Courtin, R. Depalo, A. Ertoprak, E. Fioretto, F. Galtarossa, A. Goasduff, B. Gongora Servin, A. Gottardo, A. Gozzelino, M. Heine, M. Mazzocco, R. Menegazzo, D. Mengoni, B. Million, E. Monpribat, R. Nicolás del Álamo, J. Pellumaj, R.M. Pérez Vidal, E. Pilotto, S. Pigliapoco, M. Polettini, F. Recchia, M. Rocchini, K. Rezynkina, D. Stramaccioni, S. Szilner, A. Trzcinska, J.J. Valiente Dobon, L. Zago, I. Zanon, Fusion dynamics far below the barrier for ^{12}C + ^{28}Si, Nucl. Phys. A 1063 (2025) 123195. https://doi.org/10.1016/j.nuclphysa.2025.123195

[42] N. Le Neindre, R. Bougault, S. Barlini, E. Bonnet, B. Borderie, G. Casini, A. Chbihi, P. Edelbruck, J.D. Frankland, D. Gruyer, E. Legouee, O. Lopez, P. Marini,

M. Parlog, G. Pasquali, M. Petcu, M.F. Rivet, F. Salomon, E. Vient, R. Alba, G. Baiocco, L. Bardelli, M. Bini, R. Borcea, M. Bruno, S. Carboni, M. Cinausero, I. Cruceru, M. Degerlier, J.A. Duenas, K. Gasior, F. Gramegna, A. Grzeszczuk, M. Kamuda, T. Kozik, V. Kravchuk, I. Lombardo, C. Maiolino, T. Marchi, L. Morelli, F. Negoita, A. Olmi, H. Petrascu, S. Piantelli, G. Poggi, E. Rosato, D. Santonocito, G. Spadaccini, A.A. Stefanini, T. Twarog, M. Vigilante, Comparison of charged particle identification using pulse shape discrimination and ΔE-E methods between front and rear side injection in silicon detectors, Nucl. Instr. and Meth. in Phys. Res. A 701 (2013) 145. https://doi.org/10.1016/j.nima.2012.11.005

[43] T. Kibédi, T.W. Burrows, M.B. Trzhaskovskaya, P.M. Davidson, C.W. Nestor, Evaluation of theoretical conversion coefficients using bricc, Nucl. Instrum. Methods Phys. Res., Sect. A 589 (2) (2008) 202. https://doi.org/10.1016/j.nima.2008.02.051

[44] K. Hagino, N. Rowley, A.T. Kruppa, A program for coupled-channel calculations with all order couplings for heavy-ion fusion reactions, Comp. Phys. Comm. 123 (1-3) (1999) 143–152. https://doi.org/10.1016/S0010-4655(99)00243-X

[45] O. Tanimura, Reduction of coupled equations for heavy ion reactions, Phys. Rev. C 35 (1987) 1600. https://doi.org/10.1103/PhysRevC.35.1600

[46] J. Gomez-Camacho, R.C. Johnson, Tidal symmetry in nuclear reactions: application to the scattering of polarised projectiles, J. Phys. G 12 (1986) L235. https://doi.org/10.1088/03054616/12/10/004

[47] S.R. C. W. Nestor-Jr., P. Tikkanen, Adopted values of B(E2)↑ and related quantities, At. Data and Nucl. Data Tables 78 (2001) 1. https://doi.org/10.1006/adnd.2001.0858

[48] T. Kibédi, R.H. Spear, Reduced electric-octupole transition probabilities B(E3; $0^+_1 \rightarrow 3^-_1$)–An update, At. Data and Nucl. Data Tables 80 (2002) 35. . https://doi.org/10.1006/adnd.2001.0871

[49] O. Akyüz, A. Winther, Proceedings of the International School of Physics “Enrico Fermi”, Varenna, Course LXXVII, edited by R. A. Broglia and R. A. Ricci North Holland, Amsterdam, 1981.

[50] A.M. Stefanini, G. Montagnoli, R. Silvestri, L. Corradi, S. Courtin, E. Fioretto, B. Guiot, F. Haas, D. Lebhertz, P. Mason, F. Scarlassara, S. Szilner, How does fusion hindrance show up in medium-light systems? The case of ^{48}Ca + ^{48}Ca, Phys.Lett. B 679 (2009) 95. https://doi.org/10.1016/j.physletb.2009.07.017

[51] C.L. Jiang, B.B. Back, K.E. Rehm, K. Hagino, G. Montagnoli, A.M. Stefanini, Heavy-ion fusion reactions at extreme sub-barrier energies, Eur. Phys. J. A 57 (2021) 235. https://doi.org/10.1140/epja/s10050-021-00536-2

[52] C.L. Jiang, K.E. Rehm, B.B. Back, R.V.F. Janssens, Expectations for ^{12}C and ^{16}O induced fusion cross sections at energies of astrophysical interest, Phys. Rev. C 75 (1) (2007) 015803. https://doi.org/10.1103/PhysRevC.75.015803